

Backward-wave regime and negative refraction in chiral composites

S. Tretyakov, A. Sihvola, and L. Jylhä*

Possibilities to realize a negative refraction in chiral composites in dual-phase mixtures of chiral and dipole particles is studied. It is shown that because of strong resonant interaction between chiral particles (helices) and dipoles, there is a stop band in the frequency area where the backward-wave regime is expected. The negative refraction can occur near the resonant frequency of chiral particles. Resonant chiral composites may offer a root to realization of negative-refraction effect and superlenses in the optical region.

PACS codes: 41.20.Jb, 42.70, 77.22.Ch, 77.84.Lf, 78.20.Ek

Key words: negative refraction, chiral media, effective parameters

I. INTRODUCTION

It is well known that negative refraction takes place at an interface between a usual isotropic medium (vacuum, for example) and a material with negative permittivity and permeability (called Veselago medium, double-negative material, or backward-wave medium). Recently, a lot of efforts have been devoted to realization of backward-wave materials, because the negative refraction effect offers a possibility to create super-resolution imaging devices (among other potential applications). The known realizations are based on the use of metal inclusions of various shapes, especially split rings, needed to realize negative permeability. Creation of strong artificial magnetic response, especially in the optical region, is a big challenge, which we have to face if we want to realize negative refraction and superlens for optical applications. In view of this problem, various alternative approaches to create backward-wave media have been considered in the literature. In particular, such effects can exist in more complex materials — chiral media — and, what is the key advantage, backward-wave regime can be in principle realized even if the medium has very weak or no magnetic properties. Thus, it appears that using chiral media one could realize negative refraction in the optical region without the need to create artificial magnetic materials operational in that frequency range.

The physics of the effect of backward waves in chiral media is very simple: The propagation constants of two eigenwaves in isotropic chiral media equal $\beta = (n \pm \kappa)k_0$, where $n = \sqrt{\epsilon\mu}$ is the usual refractive index, κ is the chirality parameter, and k_0 is the free-space wavenumber (see, e.g.,⁷). Near the resonance of electric or /and magnetic susceptibilities the refractive index n can become smaller than the chirality parameter κ . It means that one of the two eigenwaves is a backward wave, because its phase velocity is negative but the energy transport velocity is positive. At an interface between a usual isotropic material and such medium negative refraction takes place for this polarization (waves of the other polarization refract positively). The earliest publication where a possibility for such effects was established was probably paper¹. In that paper, a spiral model for a chiral optical molecule and the Lorentz dispersion model for the permittivity was used, and a formula for the frequency range of negative refraction was derived. Single-phase chiral substances were considered, and magnetic properties of the medium were neglected. Much more recently, backward waves and negative refraction were studied in², with the emphasis on the limiting case when both ϵ and μ tend to zero (this medium was called *chiral nihility*). The simplified antenna model for chiral inclusions³ was used to estimate the material parameters of mixtures of metal helices with the desired parameters. Possibility for backward-wave regime in chiral materials was also indicated in conference presentation⁶. In paper⁴, instead of chiral nihility, a two-phase mixture was introduced. One phase is a non-dispersive chiral material, and another phase consists of resonant dipole particles. It has been assumed that when the dipoles resonate, $\sqrt{\epsilon}$ becomes smaller than κ , and the material can support backward waves. These results show that the use of chirality is a very exciting new opportunity to realize negative refraction and related effects in the optical region in effectively uniform media (the characteristic dimensions in the material can be much smaller than the wavelength).

Chiral media have been very intensively studied in the past years, see e.g.^{7–11}. However, it is interesting, that although the possibility for this effect was published in the former Soviet Union¹, it was not known in the West until very recently. The authors of monograph⁷ thought that both eigenwaves in chiral media should be forward waves, and formulated a corresponding restriction for the material parameters [See Eq. (2.176) on page 51]. Recent studies have shown, that one of the eigenwaves in a chiral nihility is indeed a backward wave².

In this paper we study eigenwaves propagating in single- and dual-phase chiral mixtures accurately taking into account resonant properties of chiral particles and of resonating electric dipoles particles and electromagnetic interaction

between phases. We identify the effects that can lead to realization of backward-wave regime and negative refraction using chiral composites.

II. BACKWARD WAVES IN CHIRAL MEDIA AND ENHANCEMENT OF EVANESCENT FIELDS

The bi-isotropic constitutive relations read

$$\begin{pmatrix} \mathbf{D} \\ \mathbf{B} \end{pmatrix} = \begin{pmatrix} \epsilon & \xi \\ \zeta & \mu \end{pmatrix} \begin{pmatrix} \mathbf{E} \\ \mathbf{H} \end{pmatrix} = \mathbf{M} \cdot \begin{pmatrix} \mathbf{E} \\ \mathbf{H} \end{pmatrix} \quad (1)$$

where the material matrix \mathbf{M} contains the four scalars $\epsilon, \xi, \zeta, \mu$. Here we will consider only isotropic reciprocal media, in which the following condition holds⁷:

$$\zeta = -\xi = j\kappa\sqrt{\epsilon_0\mu_0} \quad (2)$$

Such media are called chiral, and κ is the chirality parameter. In lossless media κ is a real number.

Considering electromagnetic field in homogeneous chiral regions it is very convenient to introduce new field variables \mathbf{E}_\pm and \mathbf{H}_\pm that are the following linear combinations of the fields:

$$\mathbf{E}_+ = \frac{1}{2}(\mathbf{E} - j\eta\mathbf{H}), \quad \mathbf{E}_- = \frac{1}{2}(\mathbf{E} + j\eta\mathbf{H}) \quad (3)$$

$$\mathbf{H}_+ = \frac{1}{2}\left(\mathbf{H} + \frac{j}{\eta}\mathbf{E}\right), \quad \mathbf{H}_- = \left(\mathbf{H} - \frac{j}{\eta}\mathbf{E}\right) \quad (4)$$

where $\eta = \sqrt{\mu/\epsilon}$. Vectors \mathbf{E}_\pm are called wavefield vectors. The advantage of introducing the new variables comes from the fact that these new vectors satisfy the Maxwell equations in equivalent isotropic non-chiral media. This allows to use the known solutions for fields in simple isotropic medium to construct solutions for fields in chiral media.

In uniform regions the wavefield components "see" equivalent simple isotropic media with the equivalent parameters

$$\epsilon_\pm = \epsilon(1 \pm \kappa_r), \quad \mu_\pm = \mu(1 \pm \kappa_r) \quad (5)$$

where $\kappa_r = \kappa/\sqrt{\epsilon\mu}$ ⁷. The wavenumbers of the two eigenwaves read $k_\pm = k(1 \pm \kappa_r)$, or the refractive indices of the two equivalent media are $n_\pm = \sqrt{\epsilon\mu} \pm \kappa$.

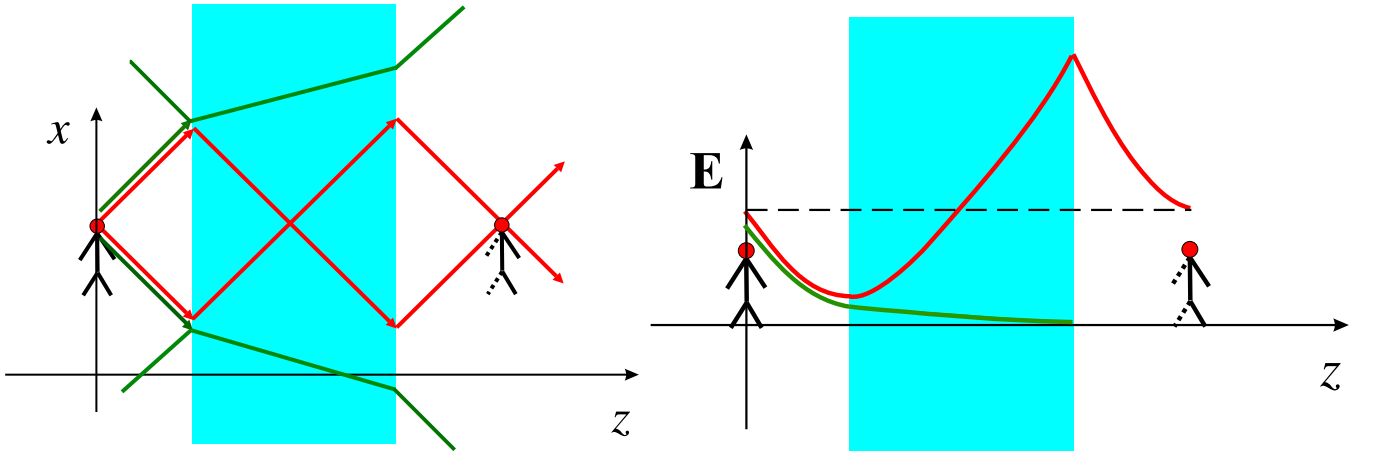


FIG. 1: An illustration of negative refraction and subwavelength focusing by a chiral slab.

Suppose that in some frequency region

$$\text{Re}\{\kappa\} > \text{Re}\{\sqrt{\epsilon\mu}\} \quad (6)$$

In this case one of the eigenmodes is a backward wave. Actually the two eigenmodes $\mathbf{E}_+, \mathbf{H}_+$ and $\mathbf{E}_-, \mathbf{H}_-$ are plane right- and left-circularly polarized waves. We see that for one of these two polarizations a slab of chiral material [when

(6) is satisfied] behaves as a slab of an isotropic medium with negative effective parameters (Veselago medium). The known phenomena of negative refraction and subwavelength focusing will take place for waves of this polarization, see an illustration in Figure 1 (These pictures have been drawn by S. Maslovski.). Numerical simulations of focusing effect have been published in¹².

The condition for creation of a perfect image for one of the two circular polarizations read

$$\epsilon_- = \epsilon(1 - \kappa_r) = -\epsilon_0, \quad \mu_- = \mu(1 - \kappa_r) = -\mu_0 \quad (n_- = -1) \quad (7)$$

III. MIXTURE OF CHIRAL AND DIPOLE PARTICLES

In⁴ it was assumed that once knowing the effective permittivity of a mixture of dipoles and the effective κ of a chiral mixture, the propagation constants of wave in a composite material which contains both types of inclusions could be calculated by a simple substitution to

$$k_{\pm} = (\sqrt{\epsilon_{\text{eff}}}\sqrt{\mu_{\text{eff}}} \pm \kappa_{\text{eff}})k_0 \quad (8)$$

where k_0 is the wave number in free space. However, this approach does not take into account electromagnetic coupling between dipoles and helices, which is rather strong near resonant frequencies of at least one phase. In this section, we introduce effective material parameters which are calculated taking this coupling into account. We assume that the mixture is built up by randomly distributed dipoles and helices in a uniform matrix with the permittivity of air. Another possibility is to construct a regular lattice of symmetrically positioned inclusions, so that the overall response is isotropic. In both cases the scattering losses from individual inclusions are supposed to be compensated, and the material can have rather low loss factor, determined only by dissipation in particles. The mixture is assumed to be dilute, in other words particles are not in each other near field, and the Clausius-Mossotti model can be used.

In the following formulation, let us use normalized field quantities: in terms of the “ordinary” electric and magnetic fields and flux densities $\mathcal{E}, \mathcal{H}, \mathcal{D}, \mathcal{B}$ with units V/m, A/m, As/m², Vs/m², respectively, we deal with fields and fluxes that are renormalized in order to have homogeneous units in each of them:

$$\mathbf{E} = \sqrt{\epsilon_0} \mathcal{E}, \quad \mathbf{H} = \sqrt{\mu_0} \mathcal{H}, \quad \mathbf{D} = \frac{\mathcal{D}}{\sqrt{\epsilon_0}}, \quad \mathbf{B} = \frac{\mathcal{B}}{\sqrt{\mu_0}} \quad (9)$$

with the free-space parameters ϵ_0, μ_0 . This leaves the materials parameters in Equation (1) dimensionless. Also, all four renormalized field quantities carry the dimension of square root of energy density: $\sqrt{\text{VAs/m}^3} = \sqrt{\text{J/m}^3}$.

A. Effective parameters

Consider a mixture where randomly oriented helices and randomly oriented dipole resonators float in neutral matrix (air). Let the polarizability matrix contribution of one element in the random distribution of helices be

$$\mathbf{A} = \begin{pmatrix} \alpha_{ee} & \alpha_{em} \\ \alpha_{me} & \alpha_{mm} \end{pmatrix} \quad (10)$$

where the averaging over spatial orientation has been included, in other words,

$$\alpha_{ee} = \frac{1}{3}(\alpha_{ee,x} + \alpha_{ee,y} + \alpha_{ee,z}), \quad \alpha_{em} = \dots \quad (11)$$

Note also that we can assume reciprocity, in other words

$$\alpha_{me} = -\alpha_{em} \quad (12)$$

[see Eq. (2)]. Of course, for lossless helices, α_{me} and α_{em} are pure imaginary.

Let the averaged polarizability matrix of the dipole resonators be

$$\mathbf{B} = \begin{pmatrix} \beta_{ee} & 0 \\ 0 & 0 \end{pmatrix} \quad (13)$$

with the similar averaging included. Here we have assumed that in addition to the vanishing magnetoelectric contribution, the magnetic response can be neglected. (This assumption is not necessary but makes the point easier to demonstrate that we can have different band behaviors for the macroscopic permittivity and chirality responses.)

Using the methods described in^{8,13}, the Maxwell Garnett formula in a matrix form for the effective parameters of the mixture can be written in the following way:

$$(\mathbf{M}_{\text{eff}} - \mathbf{I}) \cdot (\mathbf{M}_{\text{eff}} + 2\mathbf{I})^{-1} = \frac{1}{3}(n_1\mathbf{A} + n_2\mathbf{B}) \quad (14)$$

where n_1 and n_2 are the number densities of the helices and dipoles, respectively. The explicit formula for the effective parameter matrix

$$\mathbf{M}_{\text{eff}} = \begin{pmatrix} \epsilon_{\text{eff}} & \xi_{\text{eff}} \\ \zeta_{\text{eff}} & \mu_{\text{eff}} \end{pmatrix} \quad (15)$$

reads

$$\mathbf{M}_{\text{eff}} = \mathbf{I} + \left(\mathbf{I} - \frac{1}{3}(n_1\mathbf{A} + n_2\mathbf{B}) \right)^{-1} \cdot (n_1\mathbf{A} + n_2\mathbf{B}) \quad (16)$$

The resulting parameters read

$$\epsilon_{\text{eff}} = 1 + \frac{3n_1\alpha_{ee} + 3n_2\beta_{ee} - n_1^2(\alpha_{ee}\alpha_{mm} + \alpha_{em}^2) - n_1\alpha_{mm}n_2\beta_{ee}}{3 \cdot \text{DEN}} \quad (17)$$

$$\xi_{\text{eff}} = \frac{n_1\alpha_{em}}{\text{DEN}} \quad (18)$$

$$\zeta_{\text{eff}} = -\frac{n_1\alpha_{em}}{\text{DEN}} \quad (19)$$

$$\mu_{\text{eff}} = 1 + \frac{3n_1\alpha_{mm} - n_1^2(\alpha_{ee}\alpha_{mm} + \alpha_{em}^2) - n_1\alpha_{mm}n_2\beta_{ee}}{3 \cdot \text{DEN}} \quad (20)$$

where the common denominator is

$$\text{DEN} = 1 - \frac{n_1\alpha_{ee}}{3} - \frac{n_1\alpha_{mm}}{3} + \frac{n_1^2(\alpha_{ee}\alpha_{mm} + \alpha_{em}^2)}{9} - \frac{n_2\beta_{ee}}{3} + \frac{n_1\alpha_{mm}n_2\beta_{ee}}{9} \quad (21)$$

Obviously the material parameters depends on polarizabilities in a very complicate way, such that every material parameter depends on all the polarizabilities of both types of inclusions.

B. Polarizabilities of chiral inclusions

Analytical models of polarizabilities of chiral inclusions are well known in the literature, see e.g.^{3,8,10,11}. All the polarizabilities (electric, magnetic, and magneto-electric) have the resonant behaviour with the same resonant frequency which corresponds to the resonance of the whole particle. At low frequencies (well below the resonance), the electric polarizability tends to a constant, chirality parameter tends to zero linearly with the frequency, and the magnetic polarizability is proportional to frequency squared:

$$\alpha_{em} \sim j(ka)\alpha_{ee}, \quad \alpha_{mm} \sim -j(ka)\alpha_{em} \sim (ka)^2\alpha_{ee} \quad (22)$$

where a is the characteristic particle size. This brings us to the following generic model of the frequency dispersion of the polarizabilities:

$$\alpha_{em} = \frac{jAx}{1 - x^2 + j\alpha x}, \quad \alpha_{ee} = \frac{B}{1 - x^2 + j\alpha x}, \quad \alpha_{mm} = \frac{Cx^2}{1 - x^2 + j\alpha x} \quad (23)$$

where $x = \omega/\omega_0$ is the frequency normalized to the resonant frequency if the inclusion ω_0 and A, B , and C are constants.

In the optical literature, so called ‘‘hierarchy of polarizabilities’’ has been established for polarizabilities of optical molecules¹⁴. According to that, the strongest response is the electric dipole response (corresponding to the electric polarizability α_{ee} , the chirality parameter is weaker, and the magnetic dipole response is the weakest of the three

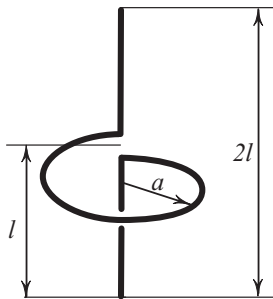


FIG. 2: The shape of the canonical helix, an illustration for the antenna model of chiral particles³.

considered here. This rule holds for usual molecules in the optical region, when the molecules are small as compared with the wavelength and spiral shapes are not very pronounced.

For our purpose we need a more general and quantitative model, that would describe particles of arbitrary relations between the length of the spiral and its diameter. To determine the relations between the polarizabilities we make use of the analytical model³ and calculate the ratios between the polarizabilities of small canonical helices shown in Figure 2. The result is

$$\alpha_{em} = j\pi \frac{a}{l} ka \alpha_{ee}, \quad \alpha_{mm} = \left(\pi \frac{a}{l} ka \right)^2 \alpha_{ee} \quad (24)$$

Here, a is the loop radius and l is the length of the dipole arm. If $ka \ll 1$ and $\pi a/l \approx 1$, we come again to the simple relations (22). However, for artificial chiral materials where the proportions between the particle dimensions can be chosen at will, and the loop radius is not always very small compared to the wavelength, we should use the more general relations (24).

Thus, we come to the following model for chiral particle polarizabilities:

$$\alpha_{em} = \frac{jx}{1 - x^2 + j\alpha x}, \quad \alpha_{ee} = \frac{\nu^{-1}}{1 - x^2 + j\alpha x}, \quad \alpha_{mm} = \frac{\nu x^2}{1 - x^2 + j\alpha x} \quad (25)$$

where we have denoted by $\nu = \pi(a/l)(ka)|_{\omega=\omega_0}$ the coefficient which depends on the electrical diameter of the spiral at resonance and on the “form-factor” (ratio of the diameter and the length of the helix). For natural optically active materials $\nu \ll 1$, but for artificial chiral materials its value can be of the order of unity.

For the electric dipole inclusions we adopt the conventional Lorentz dispersion formula, writing

$$\beta_{ee} = \frac{1}{x_0^2 - x^2 + j\alpha' x} \quad (26)$$

Here x_0 is the ratio between the resonant frequency of the dipole particles and the resonant frequency of the helices. In all expressions for the polarizabilities we omit constant (independent from the frequency) amplitude coefficients, since they can be incorporated into the number densities of chiral and dipole inclusions.

These models apply to inclusions whose dimensions are considerably smaller than the wavelength. If for example the helix radius becomes comparable to the wavelength, more complicated analytical and numerical models should be used (e.g.^{3,11}), but for the present purpose we will not need more advanced models.

IV. NUMERICAL EXAMPLES

A. The role of resonant permittivity background

Let us first calculate some numerical examples for using the simple model used in paper⁴, where the chiral material was assumed to have no frequency dispersion of the chirality parameter and the interaction between two fractions was neglected. This approximation corresponds to the frequency region well below the resonant frequency of chiral inclusions (chirality parameter is still proportional to the frequency, which we assume in our calculations, but this dependence is not of principal importance for our problem). Figure 3 illustrates typical dispersion in this frequency range for a material model of paper⁴. In this example, we have taken a very high chirality parameter, to highlight the effect of chirality (in real composites, the effect is usually pretty weak at frequencies well below the resonance).

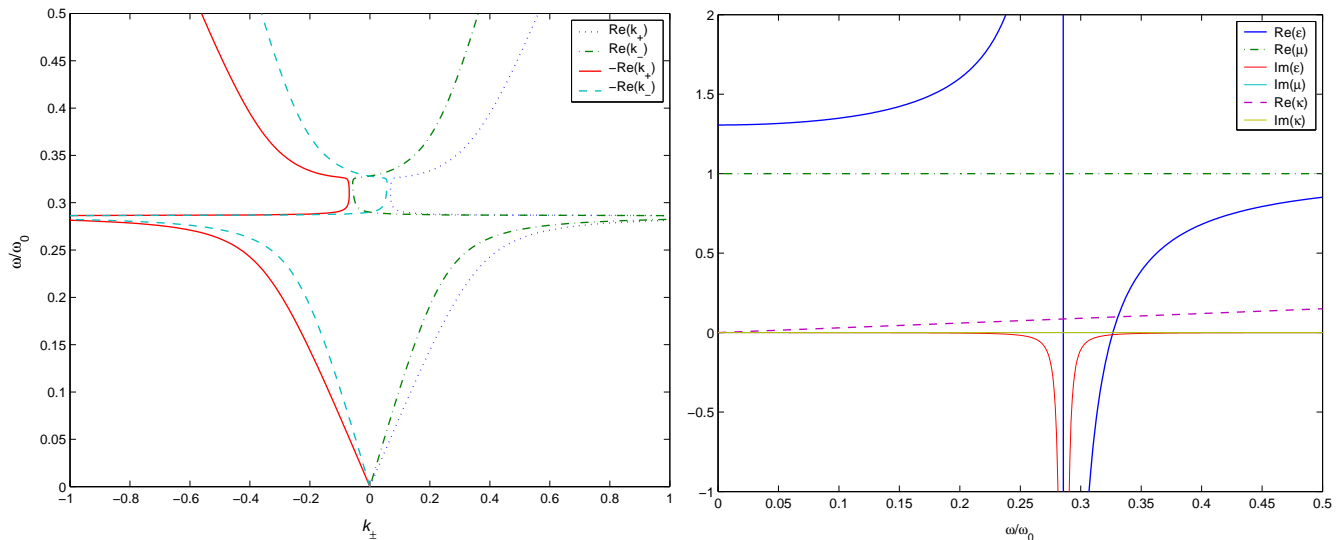


FIG. 3: Dispersion curves and effective material parameters for the Pendry model of independent fractions. $\kappa = 0.3\omega/\omega_0$. $n_2 = 0.025$, $\alpha_2 = 0.001$, resonant frequency of the dielectric phase is $0.3\omega_0$.

The chiral fraction has been assumed to be lossless. We observe that near the resonant frequency of dipole inclusions there is a very narrow backward-wave band. This effect happens when the permittivity is very small but still positive. Closer to the resonant frequency of dipoles there is a wide stop band.

However, the model used in this calculation is not realistic, because near the resonant frequencies all the material parameters resonate due to strong field interactions between particles of two phases (see Section III A). Next, we calculate an example using the model of the mixture and the particles polarizabilities introduced above.

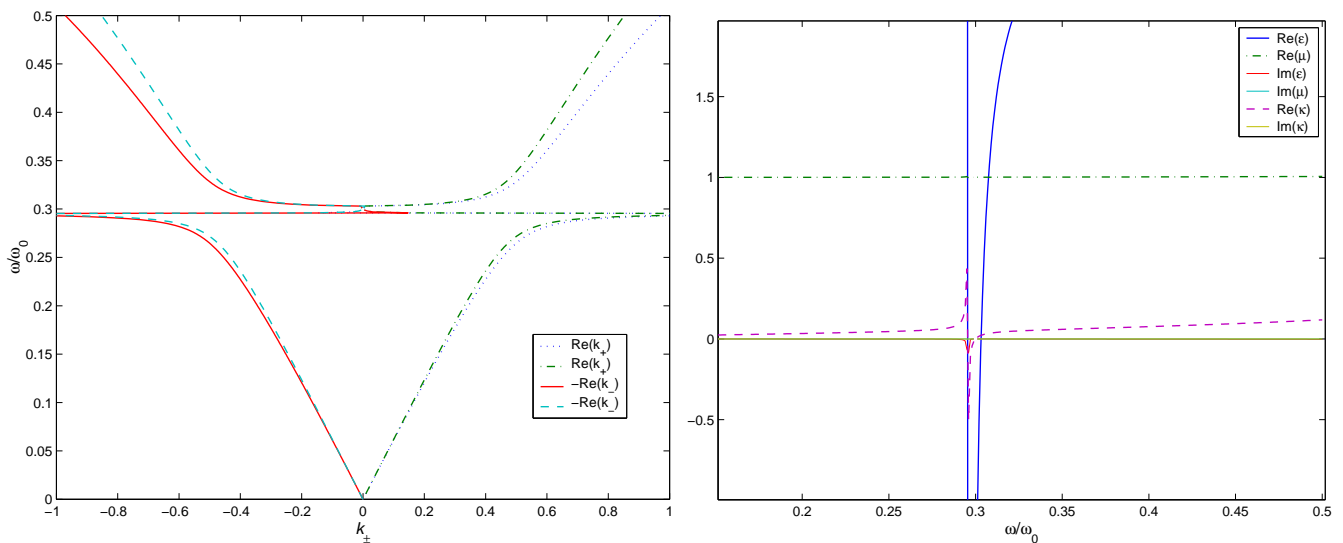


FIG. 4: Dispersion curves for a chiral medium with resonant electric dipole inclusions and its effective material parameters. The frequency is normalized to the resonant frequency ω_0 .

The resonant frequency of the electric dipole fraction is considerably lower than the resonant frequency of the helices of the chiral mixture ($0.3\omega_0$). The following parameters of the medium have been assumed: $n_1 = 0.1$, loss factor $\alpha = 0.001$, $n_2 = 0.05$, loss factor of the electric fraction particles $\alpha' = 0$. Parameter $\nu = 0.1$. In order to achieve a backward-wave effect, we assumed a very high concentration of chiral particles (in naturally available optical chiral materials the chirality parameter is usually orders of magnitude smaller) and assume that the electric dipole particles are lossless. The results are shown in Figure 4. We see that even under the above assumptions, there is actually no backward-wave band. This is apparent from the plot of the refractive indices of the two eigenmodes. The narrow

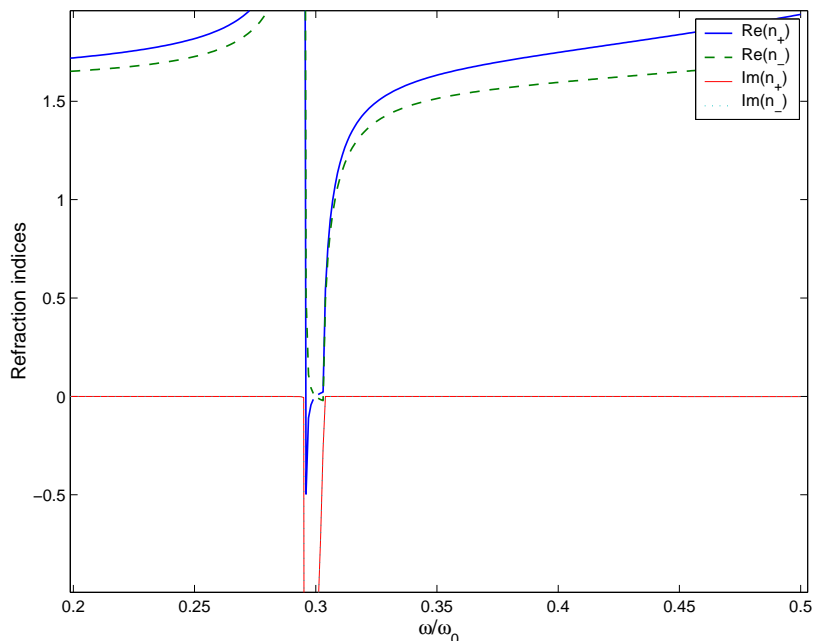


FIG. 5: Negative and imaginary parts of the refractive indices of two eigenmodes in the same medium as in Figure 4.

frequency band where the real part of one of the indices becomes negative is already inside the stop band.

Near the resonance of the electric phase all the material parameters also resonate. The resonant increase of the chirality parameter looks like a possibility to satisfy the backward-wave condition (6), because in the frequency band where the chirality parameter increases, the permittivity takes small values. However, this does not lead to a backward-wave regime. The problem is that in these two-phase composites with resonant electric dipoles embedded in a natural optically active material the effective magnetic permeability resonates very weakly. In the resonant band of the permittivity the effective permeability still stays near unity, and there is a wide stop band near the resonance of the electric phase. We have also studied the situation when the magnetic response of helical fraction is stronger, taking the value of parameter ν to be equal unity. This does not change the above conclusion, because the magnetic response considerably increases only near the resonance of the helix.

B. Interplay of the resonances of helices and dipoles

To achieve strong chiral response in practice, the working frequency should be close to the resonant frequency of chiral inclusions. Interplay of two phases becomes quite strong in this situation, and the mixture shows rather complicated frequency response. This is illustrated by numerical examples in this section.

An example of frequency dependence of effective material parameters and refractive indices is shown in Figure 6. The two phases interact strongly and all the material parameters show resonant response near the resonant frequencies of helices and dipoles. Although we assumed that helices have strong magnetic properties ($\nu = 1$), we see that predicted in⁴ backward-wave frequency band near the resonance of dipoles falls into a stop band of the mixture. Close to the resonance frequency of the effective permittivity, μ_{eff} is nearly unity and κ_{eff} also has a resonance because of coupling between dipoles and helices. It is difficult to design a backward-wave material to operate near the resonance of background permittivity because the resonances of the effective permittivity and permeability can not be tailored separately.

On the other hand, we observe that there indeed exists predicted in^{1,2} a backward-propagation band near the resonant frequency of helices.

C. Negative refraction in resonant chiral composites

The results of the previous section indicate that the most appropriate approach to realize backward-wave materials and superlenses with the use of chiral materials is the use of only chiral inclusions. In this section we give two

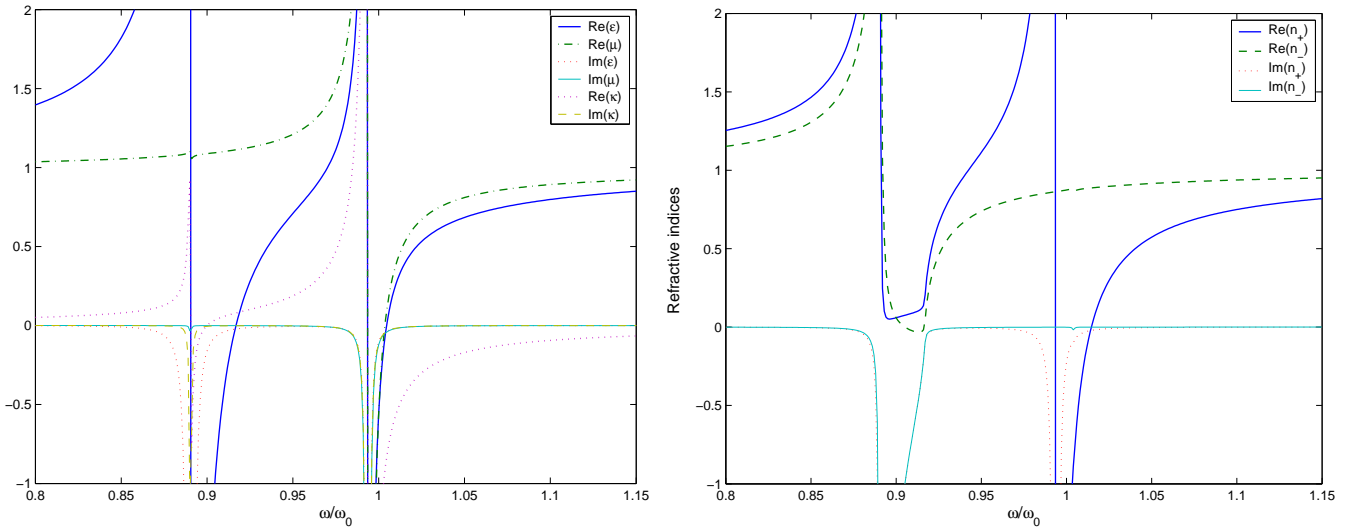


FIG. 6: Effective material parameters and refraction indices for a mixture of dipoles and helices with the parameters $n_1 = 0.02$, $n_2 = 0.05$, $\alpha = \alpha' = 0.001$, and $\nu = 1$. The resonant frequency of electric dipoles equals $0.9\omega_0$.

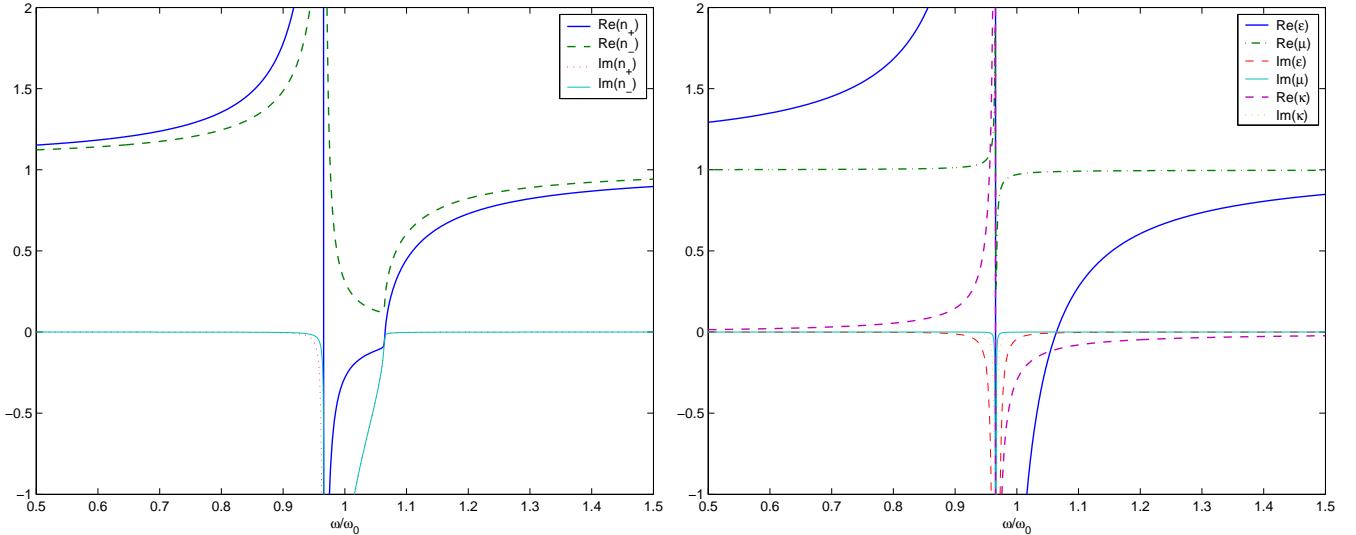


FIG. 7: Refractive indices and effective parameters of a chiral material with the parameters $n_1 = 0.02$, $\alpha = 0.001$, $\nu = 0.1$.

examples of such mixtures to illustrate the design criteria for these materials. Figure 7 gives an example of a resonant chiral material with the parameters that are probably possible to achieve using natural materials (parameter ν is much smaller than unity and magnetic properties are weak, even close to the particle resonance). This is the case first considered in¹. The results shown in Figure 7 lead to the conclusion that also here there is no propagating backward-wave regime — when the real part of the refraction index becomes negative, its imaginary part is very large.

The last Figure 8 illustrates the situation considered first in². In this case we chose a large value of parameter $\nu = 1$. The effective permeability is now much stronger due to a larger ratio of the helix diameter to its length a/l and (or) the electric diameter of the helix ka . As a result, the permittivity and permeability follow nearly the same dispersion laws, and the real part of their product remains positive even when the permittivity goes into negative. In the previous example there is a stop band in this frequency area, but in the present situation there is a propagating backward-wave regime like in the usual double-negative materials based on for example split rings and wire lattices. The role of chirality parameter here is two-fold. First, is the chirality parameter is non-zero, this backward-wave band is wider, since its limits are given by a weaker condition (6) than the usual $\text{Re}\sqrt{\epsilon\mu} < 0$. Second, the possible physical effects in this new material are reacher than in double-negative materials (see²). However, such materials do

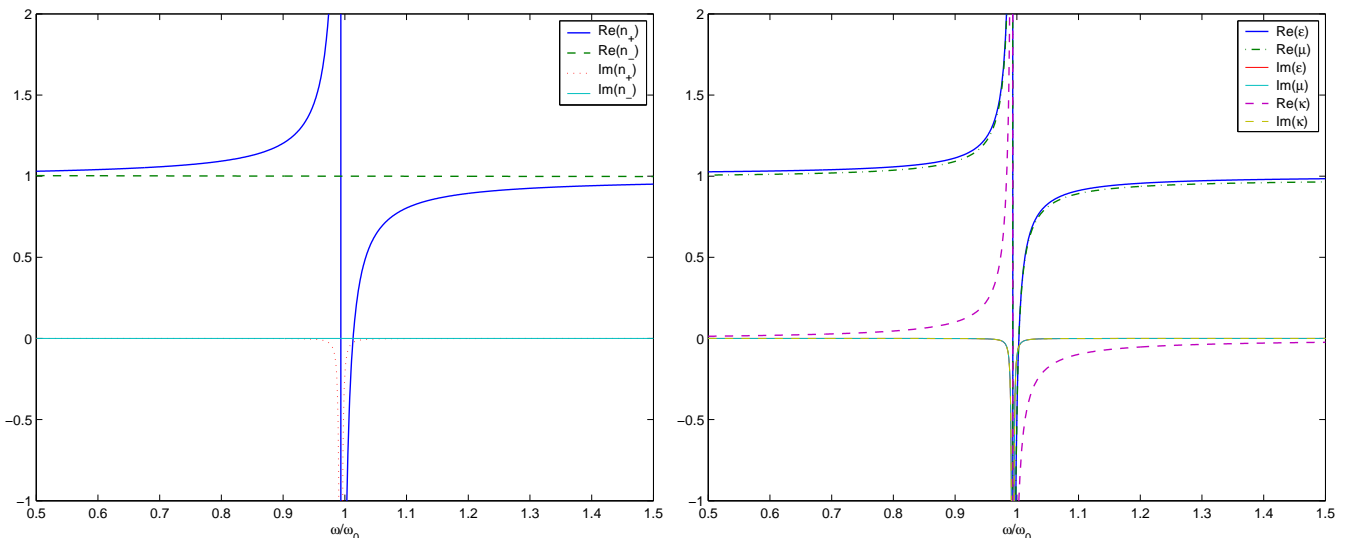


FIG. 8: Refractive indices and effective parameters of a “chiral nihility” composite material with the parameters $n_1 = 0.02$, $\alpha = 0.001$, $\nu = 1$.

not exist in nature and have to be manufactured artificially as *metamaterials*. This is reasonably easy for microwave frequencies, and there are many reports in the literature about artificial chiral media with strong resonant response (although we are not aware about any realization of the backward-wave regime). For the optical frequency range, the small required particle size makes the task very challenging, but we hope that the quickly developing nano-technologies will make it reality.

V. CONCLUSIONS

Possibilities to achieve negative refraction and enhancement of evanescent fields in a “perfect lens” using chiral materials have been theoretically explored. The two known variants have been considered: the use of a mixture of helices and resonant dipoles⁴ and the use of a composite of only helices^{1,2}. Mixing equations for the effective material parameters, which take into account the coupling between dipoles and helices has been given. Numerical examples have been calculated with the use of an introduced general dispersion law for the polarizabilities of helical particles. This model gives a possibility to study particles with different shapes and electrical sizes.

It has been shown that once the coupling between helices and dipoles is taken into account, there is a stop band in the frequency region where negative refraction was expected to occur. However, the negative refraction can still occur in a “chiral nihility” materials as has been suggested in². Negative refraction could exist at frequencies higher than the resonant frequency of chiral particles. The role of chirality is seen in widening the backward-wave frequency band and in opening a way to realize new physical effects and possibly create new microwave and optical devices. Realization of these new media for optical applications requires manufacturing of chiral inclusions with controllable shape that would exhibit resonant response in the optical regime.

* Electronic address: Sergei.Tretyakov@tkk.fi; Department Electrical and Communications Engineering
Helsinki University of Technology
P.O. 3000, FI-02015 TKK, Finland

¹ B.V. Bokut', V.V. Gvozdev, A.N. Serdyukov, Special waves in naturally gyrotropic media, *J. Applied Spectroscopy*, vol. 34, pp. 701-706, 1981.

² S. Tretyakov, I. Nefedov, A. Sihvola, S. Maslovski, C. Simovski, Waves and energy in chiral nihility, *Journal of Electromagnetic Waves and Applications*, vol. 17, no. 5, pp. 695-706, 2003.

³ S.A. Tretyakov, F. Mariotte, C.R. Simovski, T.G. Kharina, J.-P. Heliot, Analytical antenna model for chiral scatterers: Comparison with numerical and experimental data, *IEEE Transactions on Antennas and Propagation*, vol. 44, no. 7, pp. 1006-1014, 1996.

- ⁴ J. Pendry, A Chiral route to negative refraction, *Science*, vol. 306, pp. 1353-1955, 2004.
- ⁵ S. Tretyakov, I. Nefedov, A. Sihvola, S. Maslovski, C. Simovski, A metamaterial with extreme properties: The chiral nihility, *Progress in Electromagnetics Research Symposium 2003*, p. 468, Honolulu, Hawaii, USA, October 13-16, 2003.
- ⁶ H. Dakhcha, O. Ouchetto, S. Zouhdi, Chirality effects on metamaterial slabs, *Proc. of Bianisotropics'2004 — 10th Conference on Complex Media and Metamaterials*, pp. 132-135, Ghent, Belgium, September 22-24, 2004.
- ⁷ I.V. Lindell, A.H. Sihvola, S.A. Tretyakov, A.J. Viitanen, *Electromagnetic waves in chiral and bi-isotropic media*, Norwood, MA: Artech House, 1994.
- ⁸ A.N. Serdyukov, I.V. Semchenko, S.A. Tretyakov, A. Sihvola, *Electromagnetics of bi-anisotropic materials: Theory and applications*, Amsterdam: Gordon and Breach Science Publishers, 2001.
- ⁹ A. Lakhtakia, V.K. Varadan, and V.V. Varadan, *Time-Harmonic Electromagnetic Fields in Chiral Media*, Lecture Notes in Physics, 335, Berlin: Springer-Verlag, 1989.
- ¹⁰ A. Priou, A. Sihvola, S. Tretyakov, and A. Vinogradov (Eds.), *Advances in Complex Electromagnetic Materials*, Dordrecht/Boston/London: Kluwer Academic Publishers, NATO ASI Series, 3. High Technology, vol. 28, 1997.
- ¹¹ F. Mariotte, B. Sauviac, S.A. Tretyakov, Artificial bi-anisotropic composites, in *Frontiers in Electromagnetics* (ed. by D.H. Werner and R. Mittra), IEEE Press, pp. 732-770, 1999.
- ¹² Yi Jin and Sailing He, Focusing by a slab of chiral medium, 27 June 2005 / Vol. 13, No. 13 / OPTICS EXPRESS 4979.
- ¹³ A. Sihvola: *Electromagnetic Mixing Formulas and Applications*. London: IEE Publishing. Electromagnetic Wave Series 47, 1999.
- ¹⁴ R.E. Raab and O.L. de Lange, *Multiple Theory in Electromagnetism. Classical, Quantum, and Symmetry Aspects, with Applications*, Oxford Science Publications, Clarendon Press, 2005.